Finite element analysis of continuous steel casting

S. CASTAGNE, F. PASCON, G. MIESSE AND A.M. HABRAKEN

Institut de Mécanique et de Génie Civil

Université de Liège

Département M&S

Chemin des Chevreuils, 1

B-4000 Liège 1

Belgium

Anne.Habraken@ulg.ac.be
Tel : +32 – 4 – 366 9430

Fax : +32 – 4 – 366 9192

Abstract: In order to analyse the behaviour of steel during continuous casting and to improve the process, two complementary models of steel continuous casting using the finite element code LAGAMINE have been developed. We propose here a description of both macroscopic and mesoscopic approaches. The first one describes the whole continuous casting process, from the free surface in the mould and through the entire machine, including thermal and mechanical behaviour of the steel. The second approach focuses on the prediction of cracks and is developed at the grain scale. Results concerning the optimisation of the mould taper and the analysis of transverse cracks initiation are presented as industrial applications.

Keywords: *Continuous casting – Finite elements – Mould taper – Transverse cracking – Macroscopic analysis – Mesoscopic analysis*

Introduction

To improve the quality of cast products, a better understanding of the behaviour of the strand during the continuous casting process is necessary. Continuous casting can be schematically described as follows: liquid steel is poured into a bottomless copper mould that is kept at a relatively constant temperature thanks to water cooling system. Liquid steel in contact with the mould hardens and a solidified shell starts to grow (primary cooling). Under the mould, some extracting rolls pull the strand out of the mould and make it moving forward in the caster while water sprays continue cooling the strand (secondary cooling). As fast as the strand is moving down, the thickness of the solidified shell grows until the whole section is solidified. Then the strand can be cut and sent to storage.

Many parameters are important for the quality of the product. Among these parameters, we can mention casting speed, steel chemistry and cleanliness, mould taper, mould powder, mould oscillation, liquid steel temperature and the overall secondary cooling conditions. The purpose of this research is to analyse particularly the mould taper during the primary cooling and transverse cracks initiation during the secondary cooling.

In this paper, two complementary approaches of steel continuous casting modelling are proposed. The first approach consists of a macroscopic model which provides various results such as temperature field, thickness of the solidified shell, stress, strain and strain rate fields in the strand. It is used to study both primary and secondary cooling. The second approach is the development of a

mesoscopic model where the damage variable appears directly in the constitutive laws. It is dedicated to the analyse of transverse cracking.

Macroscopic approach of thermo-mechanical behaviour

Global approach

A thermo-mechanical macroscopic model has been worked out using a non-linear finite element code, called LAGAMINE, which has been developed since early eighties at the University of Liege for large strains/displacements problems, more particularly for metal forming modelling. Since a complete 3D discretization of continuous casting seemed impossible to manage (both because of numerical stability and convergence reasons, but also computing time), a 2D½ model has been preferred.
This model belongs to the "slice models" family. We can summarise the approach as follows: we model with a 2D mesh a set of material points representing a slice of the steel strand, perpendicularly to the casting direction. Initially the slice is at the meniscus level and its temperature is assumed to be uniform and equal to the casting temperature. Since this slice is moving down through the machine, we study heat transfer, stress and strain development and solidification growth, according to boundary conditions.

Mechanical model

Generalized plane strain state

From a mechanical point of view, the slice is in generalised plane strain state (2D½). That means that the thickness t of the slice is governed by the following equation:

$$t(x, y) = \alpha_0 + \alpha_1 x + \alpha_2 y \qquad (1)$$

where α_0, α_1, α_2 are degrees of freedom corresponding respectively to the thickness at the origin of the axes (α_0) and the variation of thickness along axes x (α_1) and y (α_2), both directions in the plane of the slice.
This formulation allows at the same time stresses and strains in the out-of-plane direction, which means in the casting direction. It is thus more complete than classical 2D approaches (plane strain/stress state) and much less CPU expensive than a 3D approach.
Moreover, it allows the modelling of bending and straightening of the strand, enforcing a relation between α_i degrees of freedom so that the correct radius of curvature of the machine is respected.
Last but not least, this 2D½ also permits to apply a force in the casting direction, which is of prime importance since it was necessary to take into account the withstanding force of the strand due to friction in different places in the machine.

Constitutive law

The mechanical behaviour of steel is modelled by an elastic-viscous-plastic law. The elastic part is governed by a very classical Hooke's law. In the viscous-plastic

domain, we developed a Norton-Hoff type constitutive law [1], the expression of which (in terms of Von Mises equivalent values) is:

$$\overline{\sigma} = \sqrt{3} p_2 e^{-p_1 \overline{\varepsilon}} (\sqrt{3}\dot{\overline{\varepsilon}})^{p3} \overline{\varepsilon}^{p4} \qquad (2)$$

where $p_{1,2,3,4}$ are temperature dependent parameters, which can be fitted on experimental curves. According to the assumptions of Von Mises loading surface, associated plasticity and normality in Prandtl-Reuss flow law, the expression (2) becomes in terms of deviatoric tensors:

$$\dot{\hat{\varepsilon}}_{ij}^{vp} = \frac{J_2^{p_5} e^{\frac{p_1}{p_3}\overline{\varepsilon}} \overline{\varepsilon}^{-\frac{p_4}{p_3}}}{2\left(K_0 p_2\right)^{\frac{1}{p_3}}} \hat{\sigma}_{ij} \qquad (3)$$

where $J_2 = \frac{1}{2}\hat{\sigma}_{ij}\hat{\sigma}_{ij} = \frac{1}{3}\overline{\sigma}^2$ and $p_5 = \frac{1-p_3}{2p_3}$ and the integration of this constitutive law is based on an implicit scheme. All the parameters are thermally affected.
Compression tests of cylindrical samples have been performed after a thermal treatment aiming to reproduce the thermal cycle in continuous casting. Various strain rates and temperatures have been tested and compared with simulations in order to identify the parameters of this mechanical law.

Ferrostatic pressure

The liquid pool in the middle of the strand applies a hydrostatic pressure on the solidified shell. This pressure is called ferrostatic pressure p_f and it is equal to:

$$p_f = \gamma D\left(1 - f_s\right) \qquad (4)$$

where γ is the volumetric weight of steel, D the depth under the meniscus level and f_s the solid fraction. Since the studied steel is not an eutectic composition, solidification occurs over a range of temperature limited by the solidus temperature (T_{sol}) and the liquidus one (T_{liq}). We assume a linear variation of the solid fraction according to temperature in this range:

$$0 \le f_s\left(T\right) = \frac{T_{liq} - T}{T_{liq} - T_{sol}} \le 1 \qquad \forall T \in \left[T_{liq}, T_{sol}\right] \qquad (5)$$

Since the liquid pool applies the ferrostatic pressure on the solidified shell, the strand bulges between the rolls. The maximum bulging must be controlled, otherwise the slice model gives a wrong value because of the lack of continuity in the casting direction. Some springs, the stiffness of which being fitted, allow to insert in the model a force corresponding to the shear stress in the casting direction. This way, the bulging has been controlled using the prediction of the maximum bulging based on a model taking into account the casting speed, the steel grade, the geometry and the temperature.

Thermal aspects

Internal heat conduction

The heat transfer in the material is governed by the classical Fourier's law, expressing the energy conservation and taking into account the release of energy during phase transformation (solidification is exothermic):

$$\frac{\Delta H}{\Delta T}\dot{T} = \nabla\left(\lambda \nabla T\right) \tag{6}$$

where H is the enthalpy, T the temperature and λ the thermal conductivity of the material. The enthalpy H is given by:

$$H = \int \rho\ c\ dT + \left(1 - f_s\right) L_F \tag{7}$$

where ρ is the volumetric mass, c the specific heat and L_F the latent heat of fusion.

Thermal shrinkage

Thermal shrinkage ε^{therm} due to solidification and cooling of the solid phase is given by:

$$\dot{\varepsilon}^{therm} = \alpha\left(T\right) \cdot \dot{T} \cdot I \tag{8}$$

where I is identity tensor and α is the linear thermal expansion coefficient, which is thermally affected.

Boundary conditions

Different boundary conditions can occur, according to the position of the slice in the machine and the contact conditions. Table 1 summarizes the different cases.
In case of mechanical contact, the normal pressure is calculated by allowing, but penalizing, a small penetration of bodies into each other. The friction τ_c is then computed by the Coulomb's friction law:

$$\left|\tau_c\right| = \mu \sigma_n \tag{9}$$

where μ is the friction coefficient and σ_n is the normal stress.

The heat transfer q from the strand to the ambient or the mould is given by the simple relation:

$$q = h\left(T_{strand} - T_{ambient}\right) \tag{10}$$

where h is the heat transfer coefficient according to the boundary conditions (Tableau 1). In case of contact, h is the inverse of the contact thermal resistance. In case of water spray cooling, h has been experimentally determined for different temperatures (700-1200 °C), different shapes of spray, different rates of flow and at different distances from the nozzle.

Industrial applications

Primary cooling: influence of the mould taper

A first industrial application is the study of the influence of the mould taper during the primary cooling. In case of totally convex sections such as billets and blooms, the taper should be positive on the whole outline. If the taper is too low, the contact between the strand and the mould can be lost and a gap appears leading to a decreasing thermal exchange and defects. At the opposite, if the taper is too high, friction between the strand and the mould induces stresses and strains in the solidifying shell which has a poor stiffness. For more complex cross sections (i.e. beam blanks) the taper can be negative on a part of the mould. In the same way, a wrong taper design can be responsible of quality problems.
The purpose of this study was to optimise the mould according to two criteria: maximisation of the heat quantity exchanged and minimisation of the pressure on the mould. We present here the results of the study for a billet and a beam blank.

Study of a billet

Billets have circular, squared or rectangular sections with a width/height ratio relatively small. They are devoted to long products. The product we study here is a 125-mm wide squared billet.
On Figure 1, we represent the quantity of heat exchanged between the strand and the mould for moulds whose slope vary from –3% to +3%. For the ideal taper, the heat transfer coefficient is chosen so that the mould is always in contact with the strand and no contact pressure is allowed, it corresponds to a mould that follows exactly the contraction and dilatation of the strand.
The results of Figure 1 confirm that a positive mould taper is essential to maximise the heat transfer. Nevertheless, a second criteria is necessary to compare the results between the 1% and 3% taper.
The reaction between the mould and the strand is as shown on Figure 2. According to these results, we can conclude that the taper of 1% is more favourable as the pressure on the mould is smaller.

Study of a beam blank

Beam blanks are cast products that already have a shape rather closed to the final products, i.e. I-beams. The objective was to compare single and double (Arbed) taper. The single taper has dimensions that vary linearly from the maximum to the minimum value of the real double taper mould. On Figure 3 we represent the heat quantity exchanged for three different tapers (single, Arbed and 0%) and for the ideal taper. Figure 4 shows the reaction between the strand and the mould for the three tapers.
According to the results, it is not possible to determine which taper is more favourable between the single and double taper.

Secondary cooling: study of the straightening

The purpose of the study of the secondary cooling is to evaluate the influence of some local defects (such as nozzle perturbation, roll locking or roll misalignment) on the risk of transverse crack initiation on slabs. Slabs have a rectangular section and are devoted to flat products rolling. The strain and stress history can be used

to predict damage thanks to the accumulative values of macroscopic fracture criteria implemented in the code. This is an uncoupled approach where the damage is computed from the stress and strain fields but has no influence on them. The first way to do so was to define some "macroscopic" indicators of crack initiation. We used the two following ones, both combining the gap of ductility of steel in a given range of temperature (T_A-T_B for a given steel composition) and the mechanical loadings in the direction of casting: the longitudinal stress for the first indicator I_1 and the longitudinal strain rate for the second one I_2.

$$I_1 = \begin{cases} \max\left(\sigma_{zz};0\right) & T \in \left[T_A;T_B\right] \\ 0 & T \notin \left[T_A;T_B\right] \end{cases} \tag{11}$$

$$I_2 = \begin{cases} \max\left(\dot{\varepsilon}_{zz};0\right) & T \in \left[T_A;T_B\right] \\ 0 & T \notin \left[T_A;T_B\right] \end{cases} \tag{12}$$

As it clearly appears, these indicators are different from zero only if the temperature corresponds to the range of temperature in which the ductility of the material is low and if the loading is in the sense of opening a crack (tensile stress or elongation). In such a case, the higher the loading is the higher the value of the indicators are. In any other case, the indicators are equal to zero, meaning that the risk of transverse crack initiation vanishes.

The model provides many results; among others temperature evolution (thus surface temperature, evolution of solidification, metallurgical length…), stress and strain states (and combinations such as indicators defined here above), bulging between rolls, extracting force.

Figure 5 represents a part (straightening zone) of the casting of a microalloyed steel with standard conditions (without any local defect). The figure shows the value of the 2 indicators and the localization of the maximum values (maximum risk) accords with industrial observations.

Other computations including local defects have been performed. Comparing the following reference case (standard conditions) to the value of the indicators in each defect case, we study the effect of each defect. This comparison allows us to classify the defects from the less to the most critical: nozzles perturbations are not unfavourable, one or two pairs of rolls locked is weakly unfavourable and roll misalignment is the most unfavourable.

Mesosopic model

The mesoscopic model aims at studying crack initiation and propagation in the process and especially during the unbending operation of the strand. This is a coupled approach: the damage processes are incorporated into the constitutive relations and the redistribution of stresses due to crack propagation is taken into account. The damage model uses a numerical mesoscopic approach identified by experimental measurements obtained at the microscopic and macroscopic scales. The mathematical model development begins with the construction of a 2D representative mesoscopic cell which is loaded by stress and strain fields determined by macroscopic experiments. Such an approach allows the

identification of the damage law. Concerning the application to continuous casting, the macroscopic model gives the loading (stress, strain and temperature fields) to apply to the mesoscopic cell.

Mesoscopic cell

The austenitic grain boundary is a favourable place for cracks to begin. They appear by strain concentration and microvoid coalescence at grain boundaries and by grain boundary sliding [2]. The influence of creep, controlled by diffusion, is important in the studied temperature range (between 800°C and 1000°C during the unbending phase).
In order to represent intergranular creep fracture, the developed model contains solid finite elements for the grains and interface elements for their boundaries (see also [3]). Inside the grains, an elasto-visco-plastic law without damage is used, and at their boundaries, a law with damage is preferred.
The mesoscopic approach allows a parametrical study of various factors such as grain size, precipitation state or oscillation marks geometry. The model can be applied to the continuous casting process as we know the loading to apply in the critical zone thanks to the macroscopic approach. As we want to analyse the process at the grain scale, we have to concentrate on specific zones.

Solid finite elements and grain representation

Grains are modeled by thermomechanical 4-nodes quadrilateral solid elements BLZ2T of mixed type [4]. Metallographic and texture analysis combining optical microscopy, scanning electron microscopy and orientation image microscopy, as well as various chemical etching and visual observation on steel samples, have been performed at room temperature to determine the previous austenitic grain size and morphology. Hence the geometry of the mesoscopic cell is defined taking into account the results of this micrographic study.
The Norton-Hoff law (2) is used to quantify the visco-plastic behaviour inside the grain for the studied steel.

Interface finite elements and grain boundary representation

The relevant damage mechanisms at the mesoscale are viscous grain boundary sliding, nucleation, growth and coalescence of cavities leading to microcracks. The linking-up process subsequently leads to the formation of a macroscopic crack.
The solid elements that model the grains are connected by interface elements to account for cavitation and sliding at the grain boundary. As the thickness of the grain boundary is small in comparison with the grain size, the grain boundary is represented by one-dimensional interface elements. These elements are associated with a constitutive law which includes parameters linked to the presence of precipitates, voids, etc. The damage variable explicitly appears in this law.
The interface element is composed of a modified contact element and a foundation element (Figure 6). For each integration point of the contact element, the program determines the associated foundation segment as well as the solid element to which the foundation is associated. The state variables for the interface element are computed using pieces of information of the two solids elements in

contact (elements *i* and *j* in Figure 6). The state variables in the interface element are the corresponding mean values at the integration points of elements *i* and *j*.
The original contact element is described in [5] and is usually combined with the Coulomb's friction law (9). This element has been modified in order to introduce a new interface law and a cohesion criterion. The stress components of the interface element are represented in Figure 6, their evolution is described by the following viscoelastic-type relationships:

$$\dot{\tau} = k_s \left(\dot{u} - \dot{u}_s \right) \text{ and } \dot{\sigma}_n = k_n \left(\dot{\delta} - \dot{\delta}_c \right) \tag{13}$$

This is a penalty method where penalty coefficient k_s and k_n, are very large to keep the deviations $\left(\dot{u} - \dot{u}_s \right)$ and $\left(\dot{\delta} - \dot{\delta}_c \right)$ small. $\dot{u}$ and $\dot{\delta}$ are respectively the relative sliding velocity of adjacent grains due to shear stress τ and the average separation rate, normal to the interface and the foundation, due to damage growth. These variables are directly computed from nodal displacements. The evolution of $\dot{u}_s$ and of $\dot{\delta}_c$ are computed hereafter (equations (14) and (15)). More details can be found in [6].
Grain boundary sliding is governed by:

$$\dot{u}_s = w \frac{\tau}{\eta_B} \tag{14}$$

where $\dot{u}_s$ is the relative velocity between two adjacent grains, w is the thickness of the grain boundary and η_B is the grain boundary viscosity.
The discrete cavity distribution is replaced by a continuous distribution on each facet of the grain boundary so that the cavity volume V and the average separation between two grains δ_C evolve in a continuous way on the facet (Figure 7). Then, the separation rate is given by:

$$\dot{\delta}_c = \frac{\dot{V}}{\pi b^2} - \frac{2V}{\pi b^2} \frac{\dot{b}}{b} \tag{15}$$

In this equation, the cavity volume growth rate $\dot{V}$ depends on several variables and parameters such as strain rates, stresses at the grain boundary, diffusion in the material and creep exponent. The evolution rate of the cavity spacing $\dot{b}$ is linked to the nucleation activity.
The coalescence takes place when cavities are sufficiently close to each other to collapse. At this moment, the crack begins to propagate and the interface elements are no more in contact. The parameter used to define the coalescence activation is the ratio *a/b* with *a* and *b* defined on (Figure 7). We call it a damage variable in our model. When this ratio reaches a critical value, coalescence is triggered and crack appears.
Simulations have been realised on simple representative cells in order to validate the model. Such results can be found in [6] and [7].

Meso-Macro link

Transfer of data from the macroscopic continuous casting model

Transverse cracks always appear near the edge of the slab and at its surface. So, the mesoscopic cell is chosen in this zone, perpendicular to the oscillation marks if we want to study their influence (sections 2 and 3 on Figure 8). The mesoscopic cell is surrounded by a transition zone which allows the transfer of data from the macroscopic model. It is important to follow the whole continuous casting process as we use elasto-visco-plastic constitutive laws. The history of displacements known thanks to the macroscopic simulation described in the previous section can be imposed on each node of the boundary of the transition zone as shown on Figure 9. With these boundary conditions, the crack is free to initiate in the mesosopic cell. At each time step, the temperature of each node is fixed according to the results of the macroscopic simulation and no thermal exchange is computed at this scale. Indeed, all the thermal problem has already been treated in the macroscopic model.

Identification of the interface parameters

Before applying the loading of the real continuous casting process, it is necessary to determine all the parameters of the damage law. Some of them where determined by the literature or using previous experimental results (diffusion parameter, creep parameter, grain size, …). Others have still to be identified (initial void size, initial distance between voids, nucleation parameter, …).

Description of the acoustic tests

The goal of the acoustic tests is to provide us a set of experiments to identify the parameters of the interface law. At the origin, acoustic tests were developed at the IBF in Aachen to predict the formability of steel at low temperature. They were then adapted to the condition prevalent during hot forming [8]. This is the same concept than the forming limit diagrams but here for massive sample and not for sheets.

Sets of acoustic tests are done with different sample geometry to realize different stress-strain histories at the critical point of the sample, i.e. the point where the crack will initiate. As shown on Figure 10, four geometries were used, two cylindrical (flat and slim) and two non-cylindrical (flange and concave). The samples have been compressed up to crack initiation with a constant strain rate while upcoming acoustic emission events caused by material failure have been recorded. We have tested three temperatures (800°C, 900°C and 1000°C) and two strain rates (10^{-3} s^{-1} and 10^{-4} s^{-1}). At least three samples have been tested for each combination and for each geometry to ensure a statistically relevant result.

Figure 10 shows the evolution of the specific maximal principal stress versus the effective strain at the critical point for a temperature of 900°C and a strain rate of $5\ 10^{-4}$ s^{-1}, these results have been obtained by finite element simulation of the compression test for each sample geometry. The crosses on the curves in Figure 10 indicate the moment of crack initiation. Same figures can be drawn for the other parameters combinations.

Method of identification

During the finite element simulations of Figure 10, the strain history of the critical points has been registered. This loading is applied on the mesoscopic cell of Figure 11
Figure in order to obtain the same stress-strain history. The mesoscopic cell is composed of a grain zone modelled with grains and grain boundaries and surrounded by a transition zone on the border of which the displacements are imposed.
Different combinations of the parameters are proposed and simulations are realised on the mesoscopic cell. The damage evolution in the cell is recorded and the most representative set of parameters (i.e. the one that reproduce the same damage behaviour as for the acoustic tests) is conserved. This work is still in progress.

Conclusions

Two models analysing the continuous casting process have been proposed. The macroscopic one provides results such as temperature evolution, stress and strain states for the whole process and indicators for the critical zone. For the primary cooling, the influence of the mould taper has been studied. For the secondary cooling, we have evaluated the influence of some local defects on the risk of transverse crack initiation.
The development of the mesoscopic model is still progressing. Previously, it has been shown that it is possible to follow initiation and propagation of cracks with this approach [6],[7]. Industrial practical cases will be tested as soon as the damage parameters identification will be finalized.

Acknowledgement

As Research Associate of the National Fund for Scientific Research (Belgium), A.M. Habraken thanks this Belgian research fund for its support. Industrial partner ARCELOR is also acknowledged and in particular its research teams at ARBED and IRSID and the Technical Direction of Cockreill Sambre.

References

1. Habraken, A.M., Charles, J.F., Wegria, J. and Cescotto, S. (1998) Dynamic recrystallisation during zinc rolling. Int. J. Forming Processes, 1, pp. 53-73.
2. Mintz, B., Yue, S. and Jonas, J.J., (1991) Hot ductility of steels and its relationship to the problem of transverse cracking during continuous casting. International Material Reviews, 36, pp. 187-217.
3. Onck, P. and van der Giessen, E. (1999) Growth of an initially sharp crack by grain boundary cavitation. J. Mech. Phys. Solids, 47, pp. 99-139.
4. Zhu, Y. and Cescotto, S. (1985) Unified and mixed formulation of the 4-node quadrilateral elements by assumed strain method: Application to thermomechanical problems. Int. J. Num. Meth. Eng., 38, pp. 685-716.
5. Habraken, A.M. and Cescotto, S. (1998) Contact between deformable solids: the fully coupled approach. Mathl. Comput. Modelling, 28, pp. 153-169.
6. Castagne, S., Remy, M. and Habraken, A.M. (2003) Development of a mesoscopic cell modelling the damage process in steel at elevated temperature. Key Engineering Materials, 233, pp. 145-150.
7. Castagne, S., Pascon, F., Blès, G. and Habraken, A.M. (2003) Developments in finite element simulations of continuous casting. Proc. 2nd International Conference on Thermal Process Modelling (Nancy).
8. Kopp, R. and Bernarth, J. (1999) The determination of formability for cold and hot forming conditions. Steel Research, 70, pp. 147-153.

Table 1. Boundary conditions.

position of the slice in the machine	contact conditions	mechanical boundary conditions	thermal boundary conditions
primary cooling (slice in the mould)	contact with the mould	normal stress + tangential friction	large heat transfer (direct contact)
	loss of contact	free surface (no stress)	reduced heat transfer (through the slag)
secondary cooling (under the mould)	contact with the rolls	normal stress + tangential friction	heat transfer from the strand to the rolls (direct contact)
	between the rolls	free surface (no stress)	radiation + convection or water spray or water flow

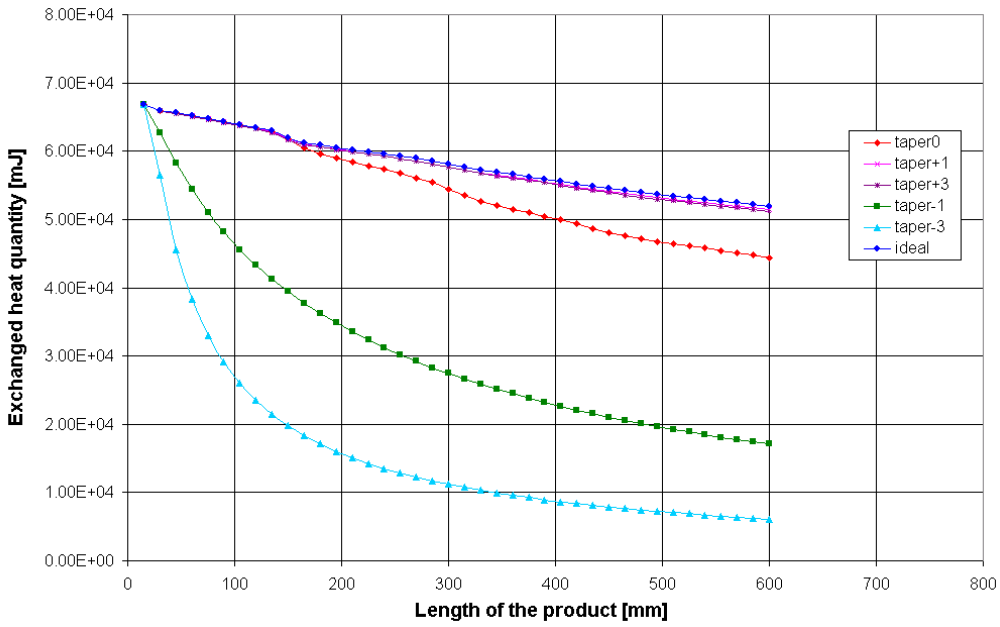

Figure 1. Exchanged heat quantity for the billet.

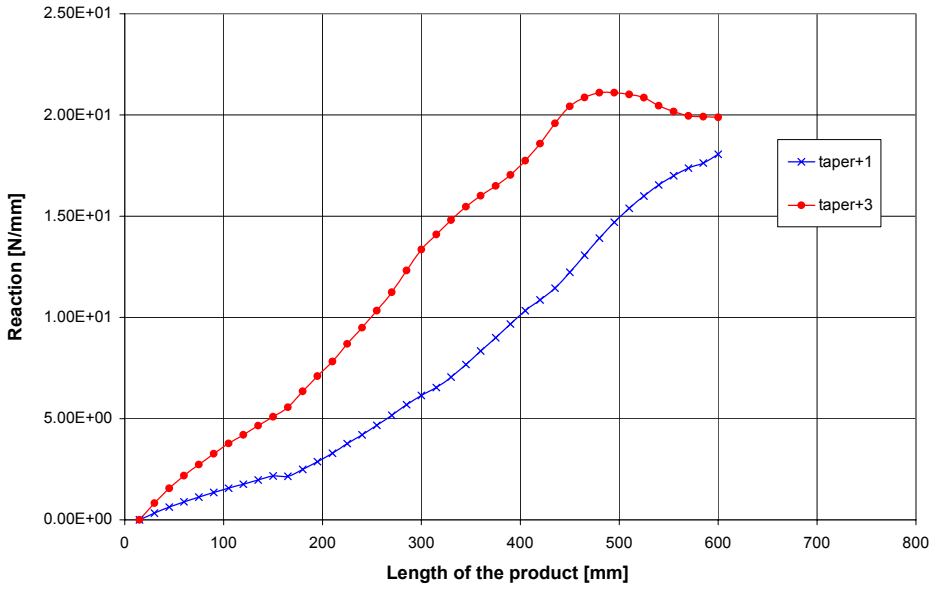

Figure 2. Reaction in the mould for the billet.

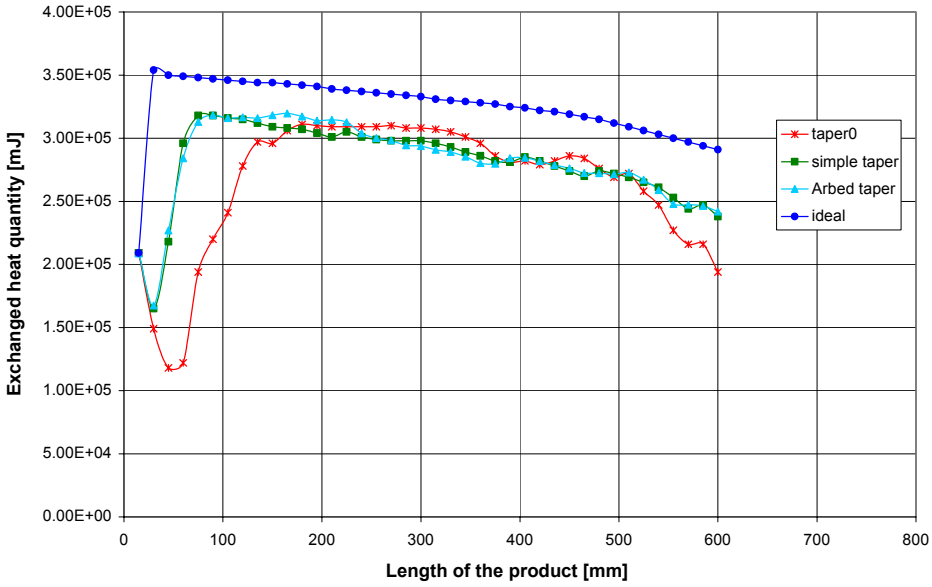

Figure 3. Exchanged heat quantity for the beam blank.

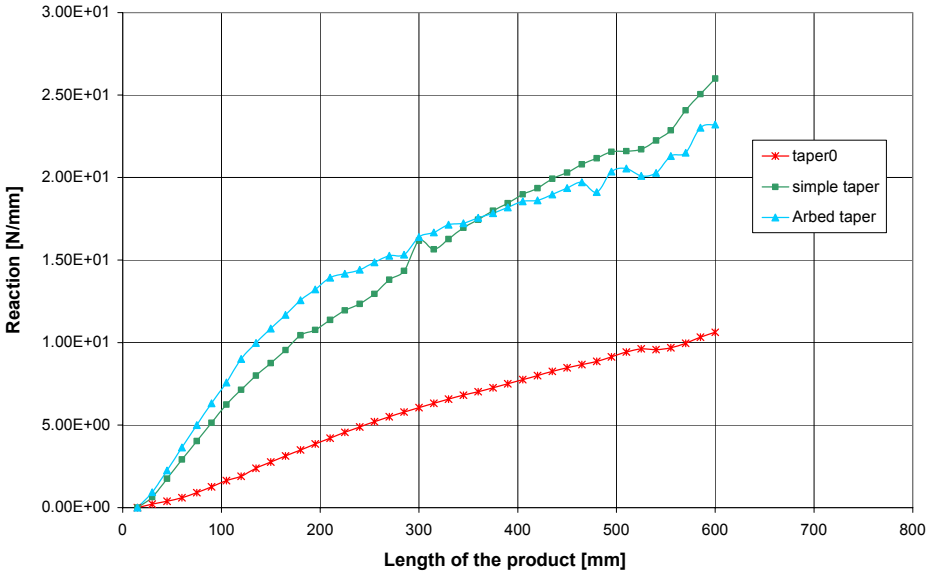

Figure 4. Reaction in the mould for the beam blank.

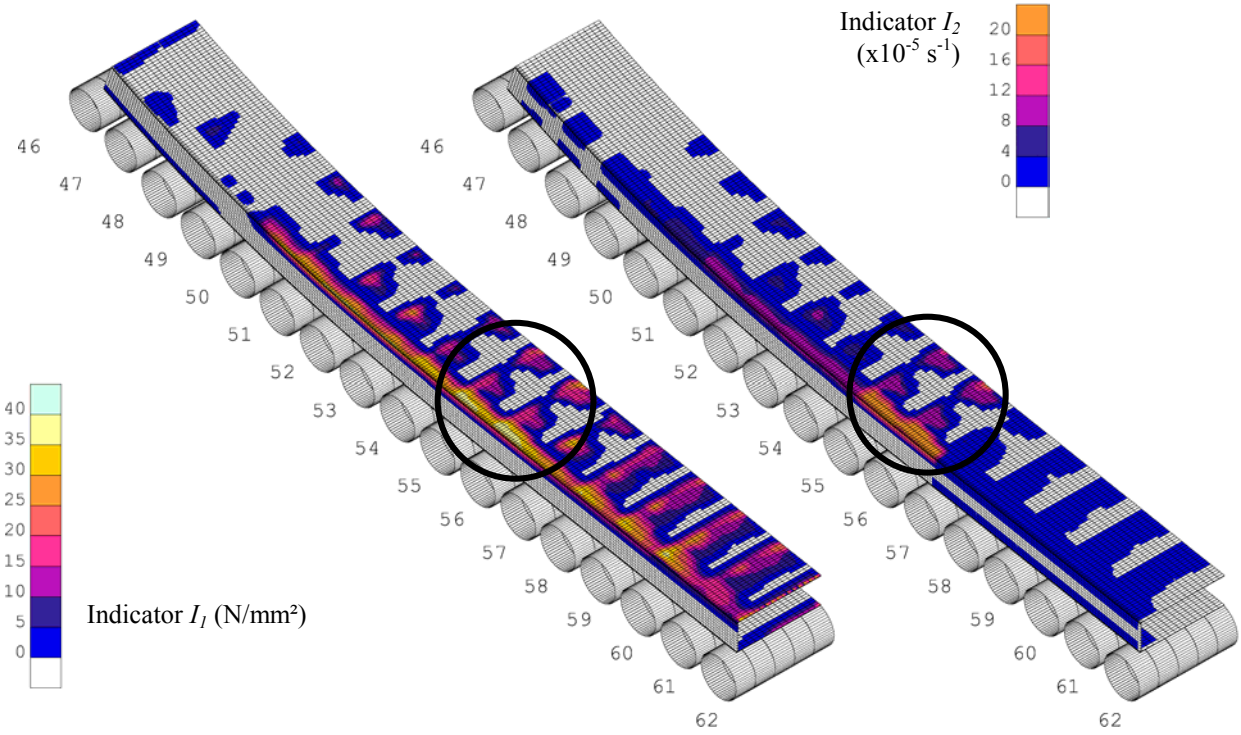

Figure 5. Indicators of risk of transverse crack initiation with standard casting conditions (reconstituted 3D view of the surface of the cast product – ½ structure because of symmetry).

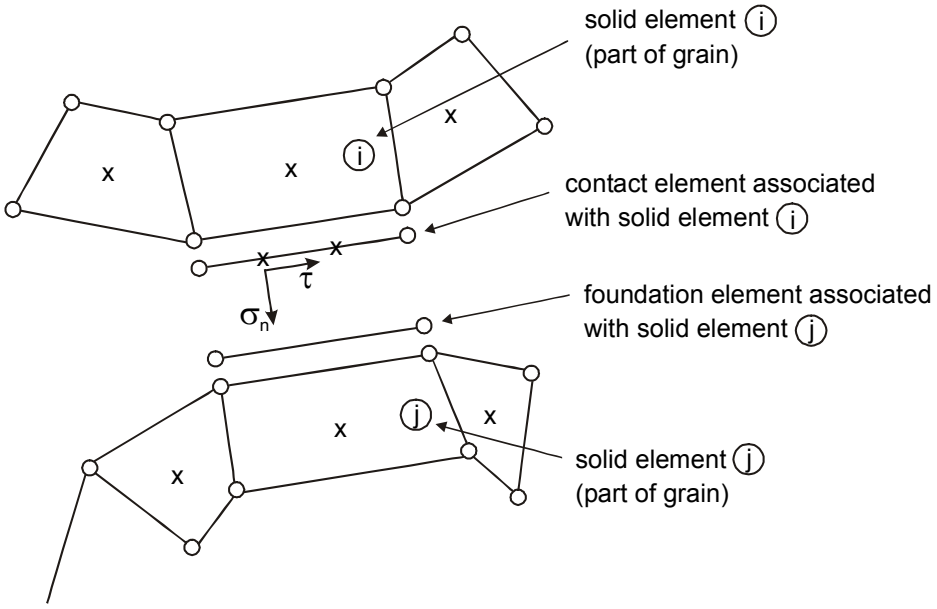

Figure 6. Interface element: contact element, associated foundation, linked solid elements. Dots symbolize nodes and crosses represent integration points.

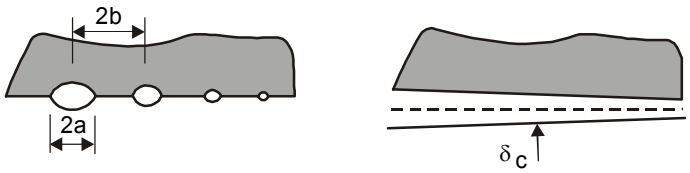

Figure 7. Discrete and continuous representations of the grain boundary.

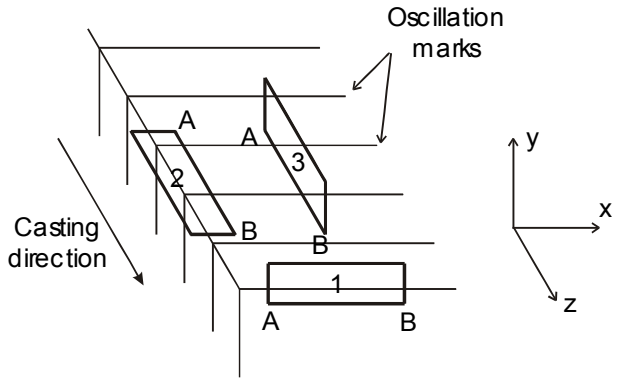

Figure 8. Piece of slab: position of the studied sections.

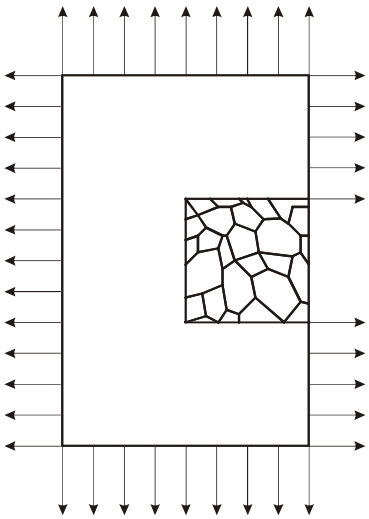

Figure 9. Mesoscopic cell surrounded by the transition zone, arrows indicate imposed displacements, oscillation marks can be introduced on the right border for sections 2 and 3.

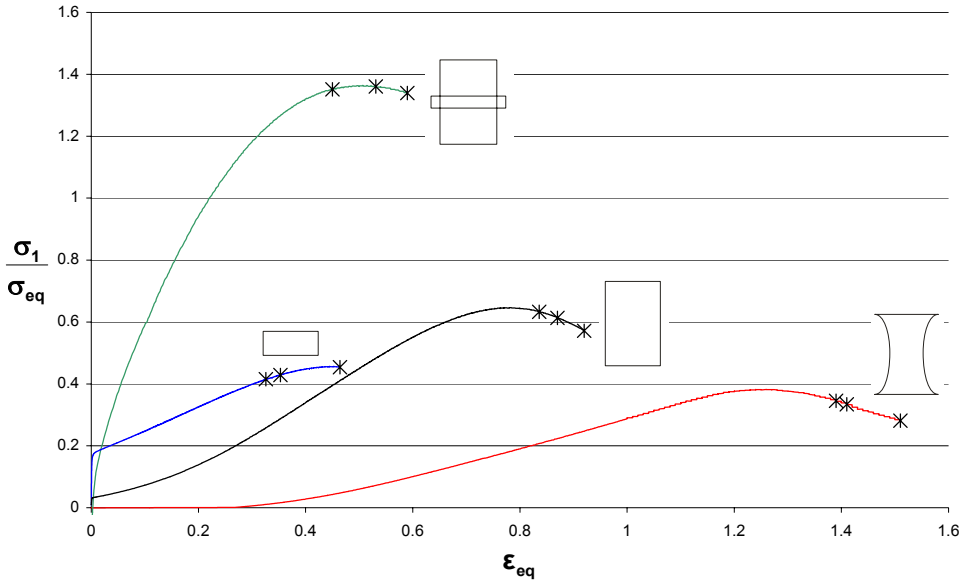

Figure 10. Acoustic cracks determination (T = 900°C, strain rate = 5 10^{-4} s^{-1}).

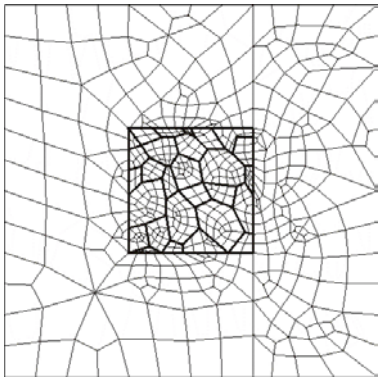

Figure 11. Mesoscopic cell used for the simulation of the acoustic tests.